Ion temperature and plasma flows in improved confinement mode in the H-1 heliac

M. G. Shats,[a)] D. L. Rudakov, R. W. Boswell, and G. G. Borg
Plasma Research Laboratory, Research School of Physical Sciences and Engineering, Australian National University, Canberra ACT 0200, Australia

(Received 20 February 1997; accepted 14 July 1997)

Low and improved confinement modes in the H-1 heliac [M. G. Shats *et al.*, Phys. Rev. Lett. **77**, 4190 (1996)] are studied experimentally in rf-sustained (<100 kW, 7 MHz) argon discharges at low magnetic fields (<0.15 T). Surprisingly high ion temperature, measured using a retarding field energy analyzer, is found which increases across the transition to improved confinement mode from 40 to 80 eV, while the electron density increases by about 50%. Both toroidal and poloidal plasma flow velocities do not change across the transition. The increase in a radial electric field in high mode is balanced on average by a corresponding increase in the ion pressure gradient. © *1997 American Institute of Physics.* [S1070-664X(97)01710-2]

I. INTRODUCTION

Transitions to improved confinement modes have been observed in a number of magnetic plasma devices. The variety of plasmas in which such transitions are observed may indicate some universal mechanism or a set of effects responsible for transitions which have been observed in a number of tokamaks,[1] stellarators,[2] and linear machines[3] in a very wide range of plasma parameters. Recently we reported the high confinement mode observed in a low electron temperature plasma in the H-1 heliac.[4] In this experiment a sudden increase in plasma density is observed when the magnetic field is close to some critical value. A new steady-state mode is characterized by a factor of (1.5–2) higher central electron density and steeper density radial gradients. The transition correlates with an increase in negative electric field and its radial shear and with a reduction in the fluctuation level and fluctuation-induced outward particle flux by a few orders of magnitude. Most of these effects, namely, the increase in the electric field shear, higher density gradients, and the turbulence suppression are commonly observed features in all types of the machines. A causality of the events during a transition has been discussed[5] and the hypothesis that a radial electric field shear ∇E_r suppresses turbulence thus leading to improved confinement is generally accepted.[6]

There are a few important questions which should be addressed with regard to the transitions in the H-1 heliac:[4]

(1) Does the energy confinement improve across the transition?

(2) What balances the observed sheared radial electric field in the two (low and high) steady states?

(3) What is the role of the plasma rotation during the transition and in steady state?

To answer these questions a study of the ion temperature and plasma flows are necessary. The role of the plasma flows in the formation of the radial electric field can be examined experimentally in terms of the radial force balance equation

$$E_r=(z_j e n_j)^{-1}\nabla P_j-\nu_{\theta j}B_\phi+\nu_{\phi j}B_\theta, \tag{1}$$

where $z_j e$ is the ion charge, n_i is the ion density, P_j is the ion pressure, $\nu_{\theta i}$ and $\nu_{\phi i}$ are the poloidal and toroidal rotation velocities, respectively, and B_θ and B_ϕ are the poloidal and toroidal components of the magnetic field. Experimental results from different machines indicate that there is no universal answer to these questions. For example, recent results from Heliotron-E stellarator[7] indicate that the increase in the radial electric field during transition to the high ion temperature mode does not coincide with any significant increase in the poloidal plasma velocity which is the case for most of the tokamak observations.[1,6] In the Wendelstein 7-AS stellarator a transition to H-mode is observed only in narrow operational windows of the rotational transform $\iota\!\!\!-$ and follows by a significant increase in the plasma poloidal rotation.[2] This observation correlates with the computed effect of the magnetic damping of the poloidal plasma rotation.[8] This damping is minimal within the same small $\iota\!\!\!-$-windows. In contrast, in the H-1 heliac, the transition is observed in a wide range of the rotational transform.[4] The conclusion about the role of the plasma rotation in the formation of the radial electric field was not possible on H-1 because of the lack of the experimental data on the ion temperature. Also, it was not clear how the energy confinement changes across the transition. In this paper we present experimental results on the transition to improved confinement in the H-1 heliac and analyze the role of the ion pressure gradient and plasma rotation in the poloidal momentum balance Eq. (1).

The paper is organized as follows: In Sec. II we describe plasma parameters and diagnostics used in this study, namely, triple probe, retarding field energy analyzer, and Mach probe. In Sec. III main experimental results are presented, including measurements of the ion and electron temperature, plasma rotation velocities, and the neutral particle density. In Sec. IV we discuss and summarize the results.

II. EXPERIMENTAL SETUP AND DIAGNOSTICS

H-1 is a three-field period toroidal heliac[9,10] (helical axis stellarator) with major radius $R_0=1.0$ m, mean minor radius $\langle a\rangle\approx 0.2$ m, externally controllable rotational transform $\iota\!\!\!-(r/a=0)=0.6-2.0$, and low vacuum magnetic field shear

[a)]Electronic mail: michael.shats@anu.edu.au

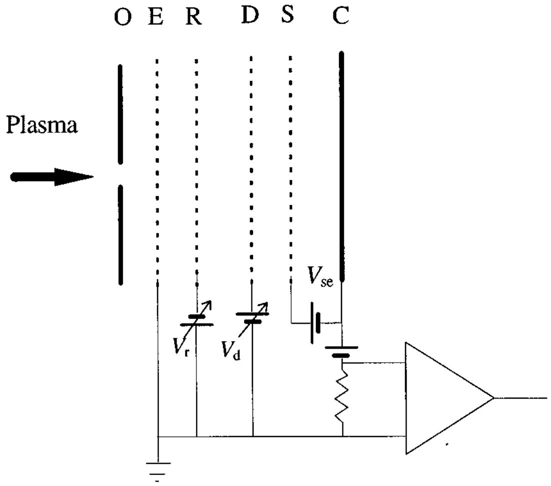

FIG. 1. RFEA bias circuit: O—orifice, E—earthed grid, R—repeller, D—discriminator, S—secondary emission suppressor, C—collector.

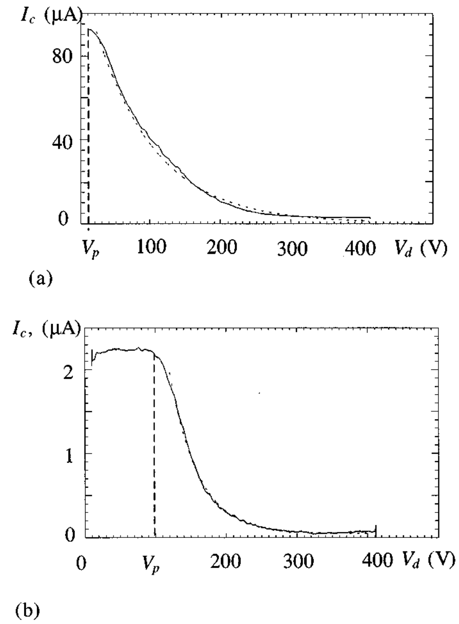

FIG. 2. $I_c(V_d)$ characteriztics measured at two different radial positions with the results of exponential fit superimposed in dashed line. (a): $r=17$ cm, $T_i=86$ eV, $V_p\approx 10$ V, (b): $r=23$ cm, $T_i=40$ eV, $V_p\approx 100$ V.

$(\Delta\iota/\iota\approx 0.03-0.06)$. A quasicontinuous operating mode at low magnetic fields ($B<0.2$ T) provides repetitive plasma pulses (pulse length about 80 ms) with up to 100 kW of rf power at 7 MHz. Plasma is produced in argon, neon, and helium. Typical plasma parameters are $n_e\sim 1\times 10^{18}$ m^{-3}, $T_e=8-30$ eV, $T_i=30-120$ eV.

Under these low electron temperature conditions a number of probe diagnostics is used. This includes a two-dimensional (2D)-scanning triple probe (electron temperature, density, plasma potential, their fluctuations and correlations), a Mach probe (ion flow velocity), a multichannel linear probe array (fluctuation phase velocity), and a retarding field energy analyzer (plasma potential, ion temperature).

The triple Langmuir probe[11,12] is used to measure the floating potential, plasma potential, electron temperature, and the ion saturation current.

The retarding field energy analyzer (RFEA) is used to measure the ion distribution function and plasma potential in the H-1 plasma. In principle, the RFEA design is similar to that used in Alcator C[13] and DITE[14] tokamaks, but uses four separate grids between the entrance slit and the collector as shown in Fig. 1. An earthed grid is placed across the entrance zone of the analyzer to define an equipotential surface and prevent the surrounding plasma perturbation by the repelling and discriminating fields of the analyzer. A repeller grid is biased negatively [typically $V_r=-(400-500)$V] in the ion mode to remove all the electrons, while the discriminator grid voltage is swept from $V_d=0-400$ V in about 10 ms. A secondary electron emission suppression grid is placed in front of the collector and is biased at $V_{\mathrm{es}}=-9$ V with respect to it. The collector current is an integral over the ion parallel distribution function:[15]

$$I_c=\frac{q}{M_i}A_{\mathrm{slit}}T\int_{q\nu_d}^{\infty}f(\nu_\parallel)dE_\parallel, \tag{2}$$

where q is the charge of the ion, A_{slit} is the input slit area, T is the grid transmission coefficient, $\nu_\parallel$ and $E_\parallel$ are the particle parallel velocity and energy, correspondingly. Typical RFEA characteristics in the H-1 plasma discharge, i.e., the ion current I_c as a function of the discriminator voltage V_d are shown in Fig. 2.

Following Ref. 16 we interpret the characteristics in Fig. 2 as being consistent with a one-dimensional Maxwellian velocity distribution shifted in velocity space by a sheath potential. The latter is equal to the plasma potential V_{pl} with respect to the probe earth. The characteristic is approximated as a function of the discriminator potential V_d:[14]

$$V\leqslant V_{\mathrm{pl}},\quad I_c(V_d)=I_0$$

and

$$V>V_{\mathrm{pl}},\quad I_c(V_d)=I_0\,\exp\left(\frac{-q(V-Vpl)}{kT_i}\right). \tag{3}$$

A least-square exponential fit (3) to the experimental characteristic gives estimates of the ion temperature and of the plasma potential.

The plasma potential measured by RFEA agrees with that measured by the triple probe to within 15% everywhere inside the last closed flux surface.

The ion velocity distribution function is derived from the RFEA characteristic[15] as

$$f(\nu)=\frac{M_i}{ATq^2}\left(-\frac{dI_c(V_d)}{dV_d}\right). \tag{4}$$

The Mach probe is used to measure plasma flow velocities. This probe consists of two identical conducting collectors (tungsten) spaced 2 mm apart which are separated by a ceramic insulator. For the measurements of the ion flows, both collectors are biased into ion saturation current. In the presence of a flow perpendicular to the probe axis the ratio of the currents drawn by the two collectors is given by

$$R = I_{si}^{+}/I_{si}^{-}, \tag{5}$$

where I_{si}^{+} and I_{si}^{-} are the ion saturation currents to the collectors facing upstream and downstream, respectively. This ratio can be related to the Mach number of the flow, $M = \nu_d / c_s$, where ν_d is a flow velocity and c_s is the ion acoustic velocity. We use a model by Hudis and Lidsky[17] for unmagnetized ions (ion Larmour radius is much bigger than a probe dimension) to relate M and R. The final relation between M and R has been modified to extend it beyond the condition $T_e \gg T_i$ used in Ref. 17, since T_i can be either higher or lower than T_e in H-1:

$$M = \frac{1}{4} \sqrt{\frac{T_e + T_i}{T_i}} \ln R. \tag{6}$$

The ion flow velocity is estimated using Eq. (6) where R is measured by the Mach probe, T_i is measured by the RFEA, and T_e is measured by the triple probe.

To justify the use of the fluid model[17] for an unmagnetized Mach probe we use an experimental procedure described in Ref. 18 to estimate the level of magnetization. The average of the ion saturation currents to the tips of the probe $(I_{si}^{+} + I_{si}^{-})/2$ does not change (within 10% of the experimental accuracy) as the probe is rotated with respect to the magnetic field. This has been checked at both the magnetic axis and near the last closed flux surface indicating a very low level of magnetization. Indeed, as will be shown in Sec. III, the ion gyroradius in our experiment is much larger (2–5 cm) than the size of the Mach probe (about 3 mm) so that the use of the model[17] seems to be justified.

III. EXPERIMENTAL RESULTS

Sudden transitions to improved confinement have been observed in H-1 in argon, neon, and helium plasmas under very similar conditions (range of magnetic fields, rf power, neutral pressure). In this paper we present experimental results obtained in the argon plasma (background filling pressure is about 3×10^{-5} Torr) in a magnetic configuration characterized by an almost zero magnetic shear and the rotational transform of $\iota\!\!\!- = 1.43$. The argon discharges are the best explored so far, though the main features of the transitions in other gases are the same: sudden (within 1 ms) jump in the average density, suppression of the fluctuations, and build-up of a strong negative radial electric field.

We refer to two steady states before and after the transition as ''low'' and ''high'' modes. This terminology does not insist on a complete similarity between the transitions observed in the H-1 plasma and those in tokamaks, though the analogy seems to be valid to a certain extent.

Radial profiles of the electron density are derived from the ion saturation current $I_s \sim n_e c_s = n_e \sqrt{(T_e + T_i)/m_i}$, electron temperature T_e (triple probe data), and ion temperature T_i (RFEA data) and are shown in Fig. 3(a) in low and high confinement modes. Density increases in the radial region of $r/a < 0.6$ and the density profile becomes steeper in the high confinement mode. The profiles in low and high modes intersect at $r/a \approx 0.62$ indicating presumably the position of the transport barrier.[5]

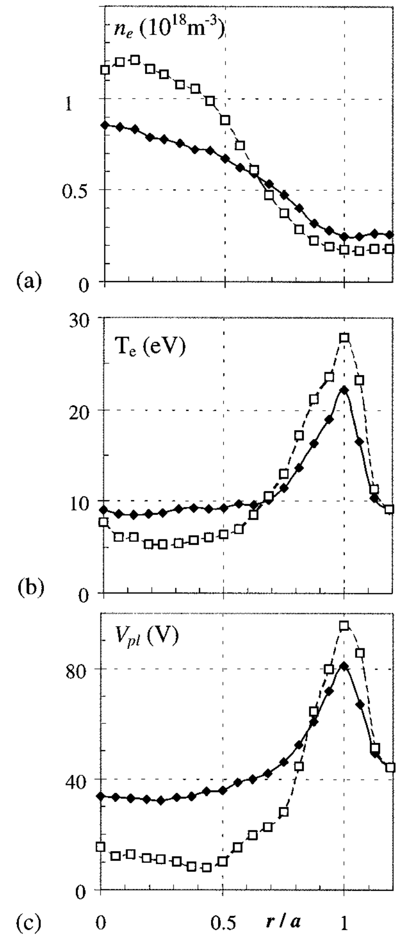

FIG. 3. Radial profiles of the electron density (a), electron temperature (b), and plasma potential (c) in low (diamonds) and high (squares) confinement modes at $P_{\mathrm{rf}} \approx 85$ kW and $p_{\mathrm{gas}} \approx 3 \times 10^{-5}$ Torr.

The electron temperature radial profiles in both regimes are hollow, as shown in Fig. 3(b). In the region $r/a < 0.6$, T_e changes from about 9 eV in low mode to 6 eV in high mode. In the region $r/a > 0.7$ the electron temperature increases after the transition from 22 eV to about 28 eV.

Plasma potential profiles computed using triple probe data as $\varphi_{\mathrm{pl}} = \varphi_f + 3.8 T_e$ (where φ_f is the floating potential) in the two regimes are presented in Fig. 3(c). Before the transition the plasma potential is about 35 V in the region $r/a \leqslant 0.6$ and increases to 80 V at the last closed flux surface (LCFS). After the transition plasma potential drops by 20 to 30 V in the region $r/a < 0.75$, while at the periphery it increases to about 100 V. The radial electric field, already negative (directed inwards) in low mode, increases after the transition by a factor of more than 2 in the region of $0.5 < r/a < 1.0$.

The ion temperature profiles measured by the RFEA are shown in Fig. 4. In low mode the ion temperature is in the range from 30 to 50 eV inside the LCFS. In high confinement mode, the ion temperature is higher everywhere in plasma, reaching $T_i \sim 90$ eV in the center of plasma.

Shown in Fig. 5(a) is the time evolution of the line-average electron density during the discharge with a spontaneous transition. Density increases by a factor of 1.3 in about 1 ms. Figure 5(b) represents the time evolution of the Mach

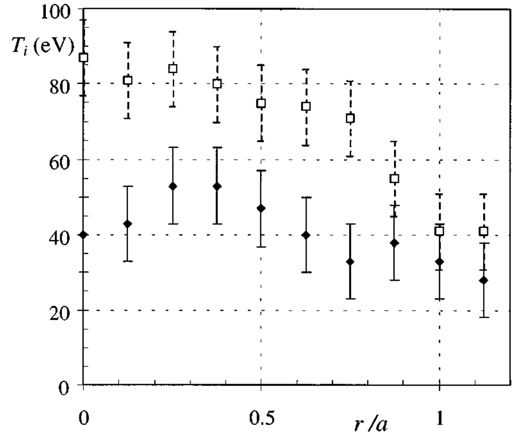

FIG. 4. Ion temperature profiles measured by the RFEA in low (diamonds, $B=0.06$ T) and high (squares, $B=0.072$ T) confinement modes at $P_{\mathrm{rf}}\approx 85$ kW and $p_{\mathrm{gas}}\approx 3\times 10^{-5}$ Torr.

probe asymmetry factor [Eq. (5)] in the poloidal direction at the radial position of the LCFS. The change in the flow asymmetry at this radius is the largest, but is still not dramatic, remaining in the range $R=1.25$–1.32 ($R=1$ corresponds to no ion flow). The radial profiles of the plasma

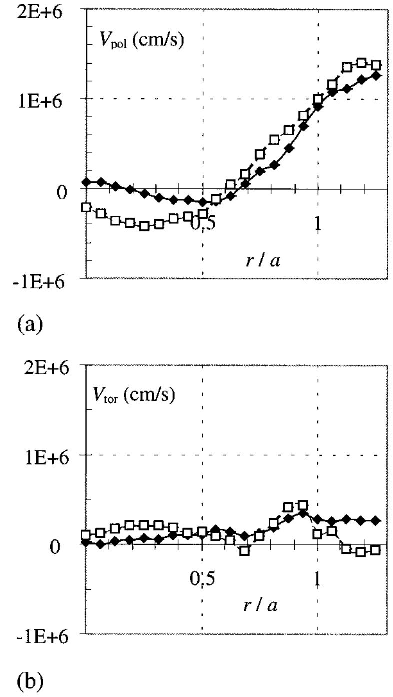

FIG. 6. Radial profiles of the plasma poloidal (a) and toroidal (b) velocity in low (diamonds) and high (squares) confinement modes at $P_{\mathrm{rf}}\approx 85$ kW and $p_{\mathrm{gas}}\approx 3\times 10^{-5}$ Torr.

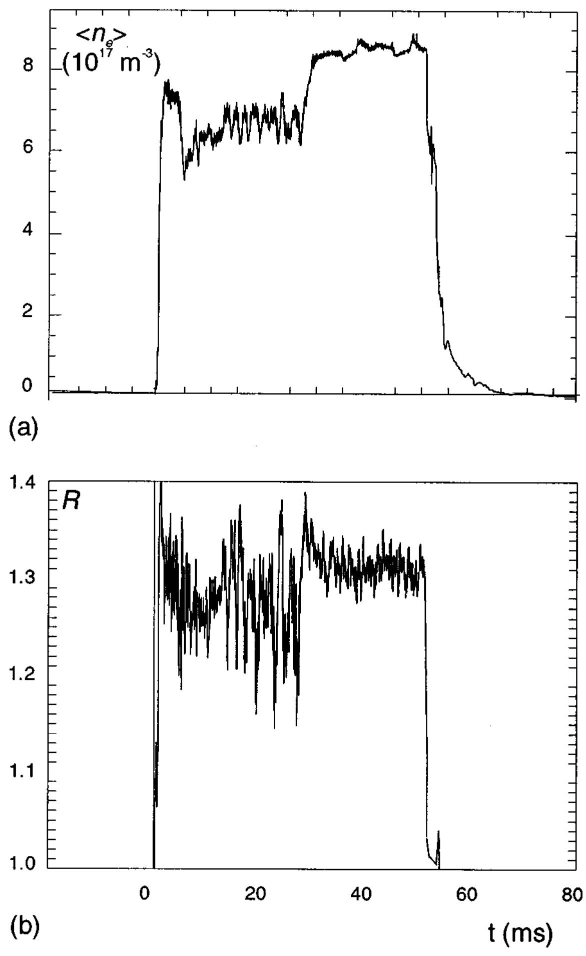

FIG. 5. Temporal evolution of the line-average density (a) and the Mach probe asymmetry factor R [Eq. (6)] at $r=23$ cm (b) in the shot with the transition to improved confinement ($B=0.061$ T, $p_{\mathrm{gas}}=3\times 10^{-5}$ Torr).

poloidal and toroidal rotation velocities before and after the transition are shown in Figs. 6(a) and 6(b). These velocities are estimated using Eq. (6) and data of Figs. 3 and 4. Both components of the plasma rotation velocity do not exceed 10^5 cm/s inside the LCFS. Negative velocities in Fig. 6(b) correspond to the direction of the $E_r\times B$ drift and of the electron diamagnetic drift in this plasma.

Spectroscopic measurements of different argon lines have been performed to estimate the ionization state of the plasma in both low and high modes of confinement. A viewing chord is scanned vertically as shown in Fig. 7(a) and the collected light is focused into the input slit of a spectrometer. The spectral line intensity is shown in Fig. 7(b) versus a viewing chord number as measured in low (diamonds) and high (squares) modes of confinement. The chord-average intensity of the argon neutral line ArI 7635 [Fig. 7(b)] is proportional to the integral $I_{\mathrm{ArI}}\sim\int n_n n_e T_e^{-1/2}\exp[-\chi_n/T_e]dl$, where n_n is the density of the neutral particles in the ground state and $\chi_n=13.1$ eV is the excitation potential for the ArI 7635 line. Experimental electron density and electron temperature profiles (triple probe data of Fig. 3) are used to unfold the spatial distribution of the neutral density from the chord-average intensities of Fig. 7(b). The neutral density shown in Fig. 8 varies inside the LCFS within a factor of 2 being maximum at $r/a=1.0$ and practically does not change in both low and high confinement modes. The ArI 7635 line intensity is lower in the high mode [Fig. 7(b)] due to the decrease in T_e in the region $r/a<0.5$ and due to the decrease in n_e at $r/a>0.6$ as shown in Fig. 3. Spectral lines of the double ionized argon ion ArIII have not been observed in this plasma suggesting $z=1$ to be a dominant ion charge state.

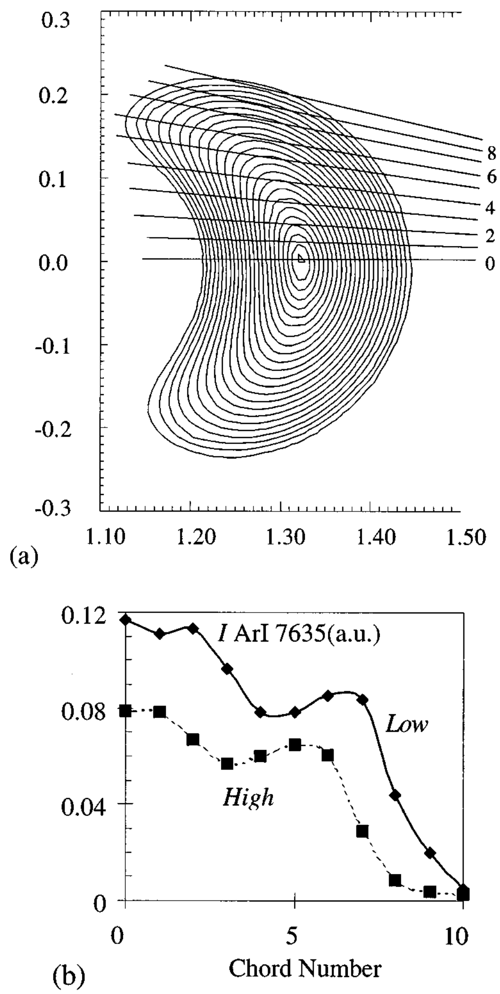

FIG. 7. Viewing chord geometry of the spectroscopic diagnostic (a) and the neutral spectral line intensity (ArI 7635 Å) versus the viewing chord number (b).

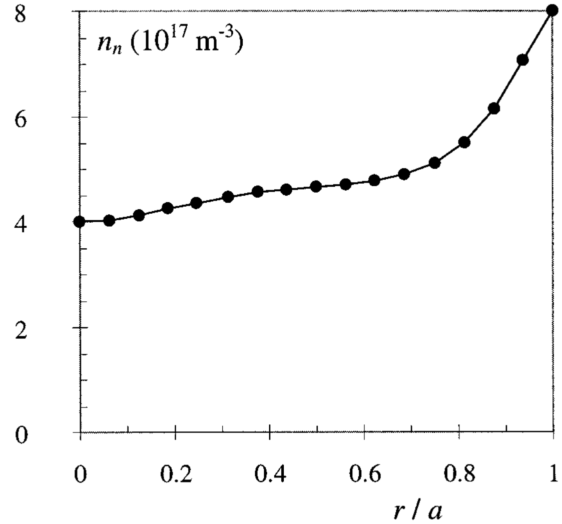

FIG. 8. Neutral density profile reconstructed from the chord-average data of Fig. 7(b) and radial profiles of Figs. 3(a) and 3(b).

IV. DISCUSSION AND CONCLUSIONS

The ion temperatures observed in both modes of confinement are significantly higher than was expected[4] for the helicon wave heating scheme[19] at the frequency of 7 MHz which is significantly higher than the ion cyclotron frequency (<60 kHz) in our experimental conditions. Experiments performed in a tandem mirror[20] have revealed similar ion temperatures to H-1 for helium plasmas produced by helicon waves under very similar plasma conditions. It is suggested,[20] that the ion heating is produced by minority heating at the ion-ion hybrid resonance introduced into the plasma at the high field points in the mirror with a hydrogen minority. Though some small (<0.5%) level of hydrogen impurity in H-1 argon or helium plasmas has been observed, the ion-ion hybrid resonance would be at 2.25 MHz on axis for a maximum field of 0.15 T. Thus the minority heating is not likely to explain high ion temperature in H-1. The ion heating mechanism is to be further investigated.

The fact that the ion temperature increases during the transition from low to high confinement indicates that the ion energy confinement improves as well as the particle confinement in the high mode. This result seems to be quite natural considering the higher than expected ion temperatures and a reduction in the fluctuation-induced particle flux by a few orders of magnitude reported in Ref. 4. The suppression of fluctuations could lead to a reduction in (at least) the convective part of the ion energy loss and the increase in the ion temperature.

The components of the radial force balance can now be estimated using data presented in Sec. III. The contribution of both poloidal and toroidal rotation to the balance [Eq. (1)] can be neglected since $V_{\mathrm{pol}}, V_{\mathrm{tor}} \ll \langle E_r \rangle / B$ ($\sim 8\times 10^5$ cm/s) everywhere inside the LCFS in both modes of confinement. Average radial electric fields estimated as $\langle E_r \rangle = [V_{\mathrm{pl}}(a) - V_{\mathrm{pl}}(0)]/a$ using data of Fig. 3(c) are $\langle E_r^L \rangle = 6$ V/cm and $\langle E_r^H \rangle = 10$ V/cm in low and high confinement modes, respectively. The ion pressure gradient term, estimated using data of Fig. 3(a) and Fig. 4 as

$$\left\langle \frac{1}{en} \frac{dp_i}{dr} \right\rangle \approx \frac{1}{e\langle n \rangle} \frac{[P_i(a) - P_i(0)]}{a},$$

is equal to 6.4 and 12 V/cm for low and high confinement modes, correspondingly. Thus averaged over the plasma radius, the radial electric field is balanced by the ion pressure gradient within the experimental error of about 20%. The detailed local radial force balance is to be further investigated, but a conclusion that the plasma rotation plays a minor role in the radial electric field formation can be made.

The observation of the relatively high intensity of the spectral line of excited neutral atoms [Fig. 7(b)] suggests the presence of the significant neutral concentration in the plasma core as shown in Fig. 8. In these conditions we estimate the steady-state ionization balance in the argon plasma in a form:

$$n_e n_n S_i - n_e n_i S_r = \nabla \cdot \Gamma, \tag{7}$$

where S_i and S_r are the ionization and recombination rate coefficients, correspondingly, and Γ is the outward particle flux. The recombination rate [second term of Eq. (7)] estimated using data on the radiative and dielectronic recombination in argon[21] is a few orders of magnitude lower than the ionization, so the ionization in these discharges is balanced by transport. Since the electron temperature in the plasma core decreases slightly across the transition, as shown in Fig. 3(b), we conclude that it is the sudden improvement in the plasma confinement rather than the ionization jump that is responsible for the significant increase in the electron density in the inner region of plasma.

Summarizing, detailed experimental studies of the transitions to improved confinement have been carried in the H-1 heliac. It is shown that:

(1) The transition is characterized by increases in the electron density and the ion temperature and by the peaking of both n_e and T_i radial profiles.

(2) The contribution of the plasma fluid rotation velocity to the radial force balance is small in both modes of confinement. Both poloidal and toroidal rotation velocities do not show any significant changes during the transition.

(3) The increase in the radial electric field after the transition is balanced on average by a corresponding increase in the ion pressure gradient term of the poloidal momentum balance equation.

ACKNOWLEDGMENTS

The authors would like to thank J. Howard, J. H. Harris, and B. D. Blackwell for the useful discussions of the results and R. Davies, G. McCluskey, J. Wach, and T. McGuiness for the operational support.

[1] K. H. Burrell, Plasma Phys. Controlled Fusion **36**, 291 (1994).
[2] F. Wagner, J. Baldzuhn, R. Brakel, R. Burhenn, V. Erckmann, T. Estrada, P. Grigull, J. H. Hartfuss, G. Herre, M. Hirsch, J. V. Hofmann, R. Jaenicke, A. Rudyj, U. Stroth, A. Weller, and the W7-AS Team Plasma Phys. Controlled Fusion **36**, A61 (1994).
[3] O. Sakai, Y. Yasaka, and R. Itatani, Phys. Rev. Lett. **70**, 4071 (1993).
[4] M. G. Shats, D. L. Rudakov, B. D. Blackwell, G. G. Borg, R. L. Dewar, S. M. Hamberger, J. Howard, and L. E. Sharp, Phys. Rev. Lett. **77**, 4190 (1996).
[5] R. A. Moyer, K. H. Burrell, T. N. Carlstrom, S. Coda, R. W. Conn, E. J. Doyle, P. Gohil, R. J. Groebner, J. Kim, R. Lehmer, W. A. Peebles, M. Porkolab, C. L. Rettig, T. L. Rhodes, R. P. Seraydarian, R. Stockdale, D. M. Thomas, G. R. Tynan, and J. G. Watkins, Phys. Plasmas **2**, 2397 (1995).
[6] K. H. Burrell, T. N. Carlstrom, S. Coda, E. J. Doyle, P. Gohil, R. J. Groebner, J. Kim, R. A. Moyer, W. A. Peebles, C. L. Rettig, T. L. Rhodes, and D. M. Thomas, Plasma Phys. Controlled Fusion **38**, 1313 (1996).
[7] K. Ida, K. Kondo, K. Nagasaki, T. Hamada, S. Hidekuma, F. Sano, H. Zushi, T. Mizuuchi, H. Okada, S. Besshou, K. Watanabe, and T. Obiki, Phys. Rev. Lett. **76**, 1268 (1996).
[8] M. Hirsch, E. Holzhauer, J. Baldzuhn, B. Branas, S. Fiedler, J. Geiger, T. Geist, P. Grigull, J. H. Hartfuss, J. Hofmann, R. Jaenicke, C. H. Konrad, J. Koponen, G. Kuhner, W. Pernreiter, A. Weller, F. Wagner, H. Wobig, and the W7-AS Team, *16th Infernational Fusion Energy Conference 1996* (to be published by the International Atomic Energy Agency, Vienna) Paper number IAEA-F1-CN-64/CP-26.
[9] S. M. Hamberger, B. D. Blackwell, L. E. Sharp, and D. B. Shenton, Fusion Technol. **17**, 123 (1990).
[10] M. G. Shats, D. L. Rudakov, B. D. Blackwell, L. E. Sharp, R. Tumlos, S. M. Hamberger, and O. I. Fedyanin, Nucl. Fusion **34**, 1653 (1994).
[11] S. Chen and T. Sekiguchi, J. Appl. Phys. **36**, 2363 (1965).
[12] M. A. Meier, G. A. Hallock, H. Y. W. Tsui, and R. D. Bengston, Rev. Sci. Instrum. **66**, 437 (1995).
[13] A. S. Wan, T. F. Yang, B. Lipschultz, and B. LaBombard, Rev. Sci. Instrum. **57**, 1542 (1986).
[14] G. F. Matthews, R. A. Pitts, G. M. McCracken, and P. C. Stangeby, Nucl. Fusion **31**, 1495 (1991).
[15] C. Bohm and J. Perrin, Rev. Sci. Instrum. **64**, 31 (1993).
[16] G. A. Emmert, R. M. Wieland, T. A. Mense, and J. N. Davidson, Phys. Fluids **23**, 803 (1980).
[17] M. Hudis and L. M. Lydsky, J. Appl. Phys. **41**, 5011 (1970).
[18] B. J. Peterson, J. N. Talmadge, D. T. Anderson, F. S. B. Anderson, and J. L. Shohet, Rev. Sci. Instrum. **66**, 437 (1995).
[19] G. G. Borg, B. D. Blackwell, S. M. Hamberger, D. Rudakov, D. A. Schneider, L. E. Sharp, M. Shats, and B. C. Zhang, Fusion Eng. Des. **26**, 191 (1995).
[20] H. Takeno, Y. Yasaka, O Sakai, and R Itatani, Nucl. Fusion **35**, 75 (1995).
[21] M. Arnaud and R. Rothenflug, Astron. Astrophys. Suppl. Ser. **60**, 425 (1985).